Cement and Concrete Research 64 (2014) 30–41

Contents lists available at ScienceDirect

Cement and Concrete Research

journal homepage: http://ees.elsevier.com/CEMCON/default.asp

Fly ash-based geopolymers: The relationship between composition, pore structure and efflorescence

Zuhua Zhang [a,*], John L. Provis [b], Andrew Reid [c], Hao Wang [a,*]

[a] Centre of Excellence in Engineered Fibre Composites (CEEFC), Faculty of Health, Engineering and Sciences, University of Southern Queensland, Toowoomba, Australia
[b] Department of Materials Science and Engineering, The University of Sheffield, Sheffield S1 3JD, United Kingdom
[c] Halok Engineering Ltd., Brisbane, Queensland 4101, Australia

ARTICLE INFO

Article history:
Received 30 January 2014
Accepted 9 June 2014
Available online 8 July 2014

Keywords:
Alkali activated cement (D)
Fly ash (D)
Carbonation (C)
Durability (C)
Pore size distribution (B)

ABSTRACT

This study reports the observation of efflorescence in fly ash-based geopolymers. The efflorescence rate strongly depends on the activation conditions; at the same alkali content under ambient temperature curing, NaOH-activated geopolymers show less and slower efflorescence than sodium silicate-activated specimens. Geopolymers synthesised at high temperature exhibit much lower efflorescence than those synthesised at low temperature, except for the sodium silicate-activated samples. The substitution of 20% fly ash by slag reduces the efflorescence rate. A relationship between alkali leaching from monosized fractured particles and 'efflorescence potential' is proposed. Soluble silicate and slag addition are beneficial in reducing efflorescence rate, but have very limited influence on the overall efflorescence potential, as they appear to have a delaying rather than mitigating effect. The partial crystallisation of geopolymers, by curing at high temperature, appears to be the most effective method of reducing the efflorescence potential.

1. Introduction

Fly ash-based geopolymers are synthesised by alkali activation of coal combustion ashes under ambient or slightly elevated temperature conditions. Because of their good workability compared to metakaolin-based geopolymers, and the availability of large volumes of fly ash in many parts of the world, fly ash-based geopolymers are beginning to be regarded as a viable alternative to Portland cement in certain construction applications, with significant reduction in environmental footprint [1,2]. In the past decade, fly ash-based geopolymer concretes produced on a laboratory scale have been widely reported to display similar engineering properties to OPC concretes [3–6], in many cases with superior mechanical properties when subjected to high temperature [7,8] or corrosive aqueous media [9,10]. However, the use of this type of material to fabricate concretes is still rare in industry compared to normal Portland cement concretes, as there exist a variety of technical, supply-chain, quality control and cost issues which pose challenges to producers [11]. Efflorescence is one such issue which has been raised as a concern in some geopolymer formulations [12]. In OPC concrete, efflorescence involves the reaction of soluble calcium with water and CO_2 to form carbonate deposits, and is generally considered harmless except for surface discolouration. However, geopolymers contain much higher soluble alkali metal concentrations than conventional cement, and so efflorescence could be a significant issue when the products are exposed to humid air or in contact with water [13].

Factors that have been reported to influence the extent of efflorescence in geopolymers include the reactivity of raw materials [14], alkali metal type [15,16] and reaction conditions [16]. Fly ashes collected from different power stations vary substantially in their chemistry and physical nature [7,17,18], and the slow reaction of some fly ash sources leads to a temptation to add excessive alkali to the mix to accelerate hardening, which can then lead to efflorescence. The addition of slag to geopolymer mixes can significantly shorten the setting time of fly ash-based geopolymers, and increase the mechanical strength at early age [19,20]. The effect of slag blending on efflorescence of geopolymers is more related to reduction in permeability rather than chemical binding of alkalis [16,21]. Najafi Kani et al. [21] proposed two possible routes to reduction of efflorescence: (1) addition of alumina-rich admixtures, and (2) hydrothermal curing. The use of 8% calcium aluminate cement as an admixture greatly reduced the mobility of alkalis in their binder systems based on a natural pozzolan; curing at ≥65 °C also provided a significant effect in efflorescence reduction [21].

Another important aspect related to the issue of efflorescence is a method to qualitatively and quantitatively evaluate the efflorescence intensity. In ASTM D7072-04 [16], for the testing of efflorescence on latex-coated substrates including concrete, it is recommended to use a tinted panel to observe and qualitatively rate the degree of efflorescence as 'none, slight, moderate or severe' on the surface facing a saturated air–water vapour mixture, based on the colour contrast between the white efflorescence product and the grey substrate. Image analysis

* Corresponding authors.
E-mail addresses: zuhua.zhang@usq.edu.au (Z. Zhang), j.provis@sheffield.ac.uk (J.L. Provis), Andrew.Reid@Haald.com.au (A. Reid), hao.wang@usq.edu.au (H. Wang).

http://dx.doi.org/10.1016/j.cemconres.2014.06.004
0008-8846/

and curettage methods can provide some quantitative information regarding the efflorescence intensity [22,23]. These methods can be classified as direct methods. Indirect methods are also adopted by researchers to qualitatively evaluate the efflorescence of construction materials including geopolymers [15,16,21]. There is not an extensive body of direct information available to connect these indirect methods to service conditions for prediction of efflorescence in service, as the samples and exposure conditions are different, and the cyclic exposure conditions experienced in many service applications also add complexity to the analysis. The development of a validated, rapid method to provide quantitative prediction of efflorescence is undoubtedly needed.

The aims of this research are therefore to study the effects of typical manufacturing factors on efflorescence of geopolymers, using both direct and indirect methods. The efflorescence on the surface of geopolymers in contact with water is observed and recorded by a digital camera, as a direct method, with comparison to the indirect method of measurement of the alkali concentrations and pH of leaching solutions. A better understanding of the relationship between composition, structure and efflorescence of this type of materials is achieved by the X-ray diffraction (XRD), porosimetry (MIP) and leaching analysis of geopolymers as a function of fly ash sources and curing conditions.

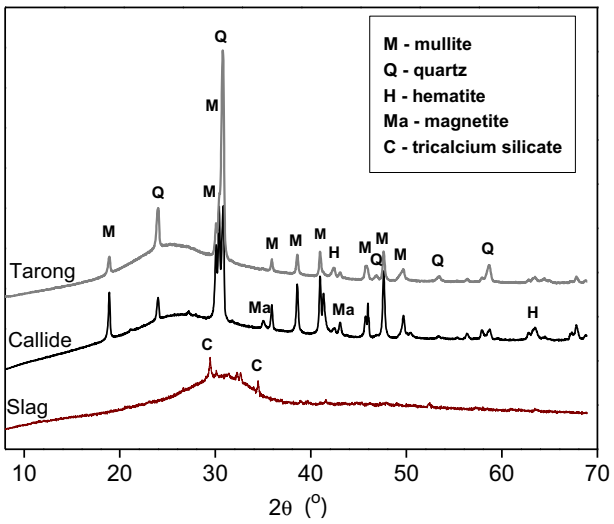

Fig. 1. XRD pattern of fly ashes and slag, in Tarong fly ash: mullite, $Al_{4.75}Si_{1.25}O_{9.63}$ (ICSD# 66448), quartz, SiO_2 (ICSD# 89280); magnetite, Fe_3O_4 (ICSD# 43001); in Callide fly ash: mullite — $Al_{1.83}Si_{1.08}O_{4.85}$ (ICSD# 43298), quartz — SiO_2 (ICSD# 89280), magnetite — Fe_3O_4 (ICSD# 43001), hematite — Fe_2O_3 (ICSD# 15840); in slag: tricalcium silicate — Ca_3SiO_5 (ICSD# 81100).

2. Materials and methods

2.1. Materials

Fly ashes obtained from Callide and Tarong Power stations in Queensland, Australia were used to manufacture geopolymers. This allows a comparison of the effects of fly ash properties on efflorescence. Granulated blast furnace slag was used as a secondary calcium source. The chemical compositions of the fly ashes and slag were determined by X-ray fluorescence (XRF), and are shown in Table 1. Both fly ashes are Class F according to ASTM C618.

The fly ashes and slag were examined by XRD, Fig. 1, using an ARL 9900 Series X-ray workstation with Co Kα radiation, operated at 40 kV and 40 mA, with a step size of 0.02° and a count time of 1 s/step. Further analysis by the Rietveld quantitative XRD method with corundum as an internal standard [24] shows that Callide ash contains 15.3% mullite, 6.5% quartz, 2.4% magnetite and the balance amorphous; Tarong ash contains 24.1% mullite, 13.1% quartz and the balance amorphous; and the slag contains >95% amorphous glass. The trace amount of tricalcium silicate observed in the slag may come from contamination by Portland cement during grinding or transportation. The particle size distributions of the three solid precursors were determined using a Malvern Mastersizer 2000, Fig. 2. The surface areas of Callide and Tarong ashes, and the slag used, are estimated by this method to be 0.94, 0.64 and 0.69 m^2/g, respectively.

The activators used were NaOH solution and two sodium silicate solutions. The NaOH solution was prepared by dissolving NaOH pellets (99% purity, Taiwan Alum Chemical Industrial Co., Ltd.) in water to a concentration of 12 mol/L, and cooled to room temperature. One sodium silicate solution was D-Grade™ liquid sodium silicate (PQ Australia) with Ms (molar ratio SiO_2/Na_2O) = 2.0 (Na_2O = 14.7 wt.%, SiO_2 = 29.4 wt.%), and the other was a mixture of this commercial sodium silicate with NaOH solution to give a combined modulus of Ms = 1.5 (Na_2O = 16.6 wt.%, SiO_2 = 24.1 wt.%). The solution was allowed to cool and equilibrate for at least 3 h prior to use.

Table 1
Compositions of fly ash and slag as determined by XRF. LOI is loss on ignition at 1000 °C. Att values in wt.%.

	SiO_2	Al_2O_3	CaO	MgO	K_2O	Na_2O	Fe_2O_3	P_2O_5	SO_3	TiO_2	LOI
Callide	54.4	32.1	1.1	0.8	0.2	0.1	7.5	0.1	≤0.1	2.1	0.8
Tarong	72.1	24.7	0.1	0.18	0.5	≤0.1	1.2	≤0.1	≤0.1	1.4	0.4
Slag	33.3	14.6	41.7	6.1	0.3	0.2	0.8	0.2	0.6	0.6	0.5

2.2. Geopolymer manufacture

Geopolymer specimens were manufactured by adding the activator solutions to the solid precursor (fly ash, or blended fly ash and slag) at a constant Na_2O/precursor mass ratio of 5.8% in Callide ash mixtures and 6.5% in Tarong ash mixtures. The higher alkali content in the latter mixtures was required to achieve acceptable strengths (Table 2). The minimal required amount of additional water was added during mixing to achieve a suitable workability.

Table 2 shows the mix proportions and curing conditions of geopolymers, and their compressive strengths. The pastes were poured into ø23 mm × 24 mm cylindrical moulds and subjected to humid curing with RH > 90% at 25 ± 2 °C for 24 h. The demoulded specimens were further aged at high temperature (80 ± 1 °C) and

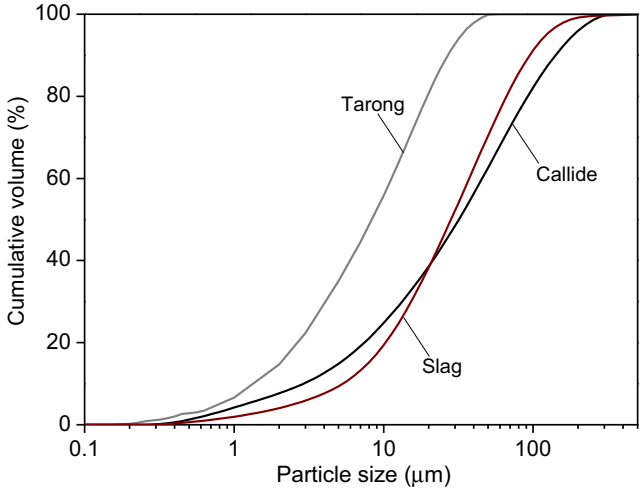

Fig. 2. Particle size distribution of Callide and Tarong fly ashes and slag.

Table 2
Mix proportions and curing conditions of the geopolymers, and their compressive strengths at 90 d. Compressive strength is reported as mean and standard deviation among 6 replicate specimens.

Mixtures	Fly ash (g)	Slag (g)	Activator solutions (g)		Foam (g)	Curing s cheme	Compressive strength (MPa)
	Callide		*12 M NaOH*	$Na_2O{\cdot}1.5SiO_2$			
CL1L	100	0	23.1	0	0	23 °C × 90 d	4.0 ± 0.3
CL1H	100	0	23.1	0	0	80 °C × 90 d	26.2 ± 2.1
CL2L	100	0	0	35	0	23 °C × 90 d	53.2 ± 0.9
CL2H	100	0	0	35	0	80 °C × 90 d	58.4 ± 12.1
CLSL	80	20	0	35	0	23 °C × 90 d	77.4 ± 7.0
CLSH	80	20	0	35	0	80 °C × 90 d	58.2 ± 11.2
	Tarong		*12 M NaOH*	$Na_2O{\cdot}2.0SiO_2$			
TR	100	0	15.5	24	0	23 °C × 90 d	26.0 ± 1.5
TRF	100	0	15.5	24	5	23 °C × 90 d	4.5 ± 0.5
TRSF0	70	30	15.5	24	0	23 °C × 90 d	48.5 ± 2.1
TRSF1	70	30	15.5	24	3.3	23 °C × 90 d	16.2 ± 3.3
TRSF2	70	30	15.5	24	5	23 °C × 90 d	12.3 ± 1.2
TRSF3	70	30	15.5	24	16	23 °C × 90 d	3.4 ± 0.7

ambient temperature (23 ± 3 °C) in sealed glass containers. To provide humid conditions, the containers contained water at the bottom but not in contact with the specimens. Foamed geopolymers were also manufactured to examine the effects of pore structure on the efflorescence. Pre-foaming was achieved by the use of a foam generator using a synthetic organic foaming agent, which was then mixed with the fresh paste. The foamed pastes were poured into ø53 mm × 108 mm polypropylene moulds, sealed and cured at 40 °C for 24 h, then aged at room temperature for 90 d.

2.3. Testing and characterisation

The compressive strength of hardened samples was tested at 90 d using an MTS universal mechanical testing machine. The loading speed was 0.5 mm/min. Before testing, the top surfaces of the cylindrical specimens were sanded to be flat and parallel, at a diameter to height ratio of 1:1 for the dense samples and 1:2 for the foamed samples. The compressive strength testing results are given in Table 2.

To observe the severity of efflorescence, the 90 d-aged geopolymer samples were put in contact with water at the bottom (constantly immersed at 1 mm depth) under ambient conditions with 23 ± 3 °C and RH = 67 ± 28%. The white efflorescence product scraped from the surface after 7 d was analysed by XRD as described above.

To quantify the efflorescence potential, the leaching of alkali metals was investigated. The 90 d-aged samples were crushed and sieved. Particles between 1.25 and 1.50 mm were collected, mixed with deionised water at a solid/water mass ratio of 1:50, sealed and stored at 25 ± 2 °C under laboratory conditions. Aliquots of 20 mL of the supernatant solution were removed after 3, 6, 12, 24 and 96 h, filtered and diluted with deionised water in a ratio of 1:25. This diluted solution gave suitable Na^+ and K^+ concentrations for atomic absorption spectroscopy (AAS, AA-7000) analysis. The pH of the leaching solution was also measured using a MeterLab ION 450 pH analyser.

To understand the factors that influence efflorescence, selected samples were analysed by XRD, thermogravimetric analysis (TGA), scanning electron microscopy (SEM), and mercury intrusion porosimetry (MIP). TGA was performed using a Q500 instrument at a heating rate of 10 °C/min from 25 °C to 900 °C in air to provide information regarding the quantity of bound water, which was used in quantifying the alkali leaching extent. The samples were all dried at 105 °C for 6 h. This pre-conditioning was for a simple standardisation purpose, rather than to completely evaporate free water present in the samples. The pore structure of the solid samples was analysed by MIP. Since the sample drying process may affect MIP testing results to a significant extent [25], careful sampling was performed. The specimens were first crushed into pieces around 3 × 3 × 3 mm in size, then stored in acetone for at least 24 h to remove the pore water. After being dried at 65 ± 2 °C for at least 6 h, the samples were transferred into a desiccator until testing. The testing was performed using a Poremaster GT-60 MIP (Quantachrome), with the surface tension of mercury taken as 0.48 N/m and contact angle 140° for all calculations, which is typical in cement MIP analysis [26] and was also adopted in a previous study of metakaolin-based geopolymers [27]. Since the high pressure of mercury intrusion would be expected to damage the microstructure of the foamed geopolymers, the porosity of foamed samples was determined by water saturation under a vacuum of −80 to −100 kPa. SEM analysis of fractured samples dried by the same method (65 °C × 6 h) was conducted on an EVO MA18 40XVP instrument, to enable direct comparison of the pore structure of solid and foamed samples. The accelerating voltage used was 20 kV, and the samples were coated with Au. The porosity and pore size of the foamed samples were also analysed by an image analysis (IA) system consisting of an Olympus optical microscope and the Analysis-FIVE software. The sample preparation was undertaken according to the method proposed by Nambiar and Ramamurthy [28]. Briefly, polished surfaces of samples were tinted with black ink and then the open pores on the surface were filled with talc powder. This process provided a surface with sharp and easily distinguishable boundaries of the voids and matrix, visible by their high colour contrast under optical microscopy.

3. Results

3.1. Visual observation of efflorescence

Figs. 3 and 4 show visible formation of efflorescence on the surfaces of geopolymers. The 23 °C sealed aged geopolymers CL1L and CL2L exhibit rapid efflorescence, which is visible after 3 h (not shown here) and the white products become thicker after 6 h (Fig. 3). In comparison, the 80 °C hydrothermal aged geopolymers exhibit much slower efflorescence rates (Fig. 4), and efflorescence products are not observable with the naked eye on either CL2H or CLSH after 6 h. It is noted that CLSL specimens (cured at 23 °C, with slag addition) do not show efflorescence after 24 h in contact with water, similar to the 80 °C hydrothermal aged specimens. The observation that hydrothermal curing can reduce efflorescence is consistent with the results of Najafi Kani et al. [21].

Fig. 5 shows the efflorescence of solid geopolymer TRS0 and the corresponding foamed product TRS2. It seems from these images that a higher porosity hinders the rapid visible efflorescence of efflorescence product. This is in contrast to the common understanding that a porous structure provides more channels for the transport of water and alkali cations, which would be expected to lead to efflorescence. The large

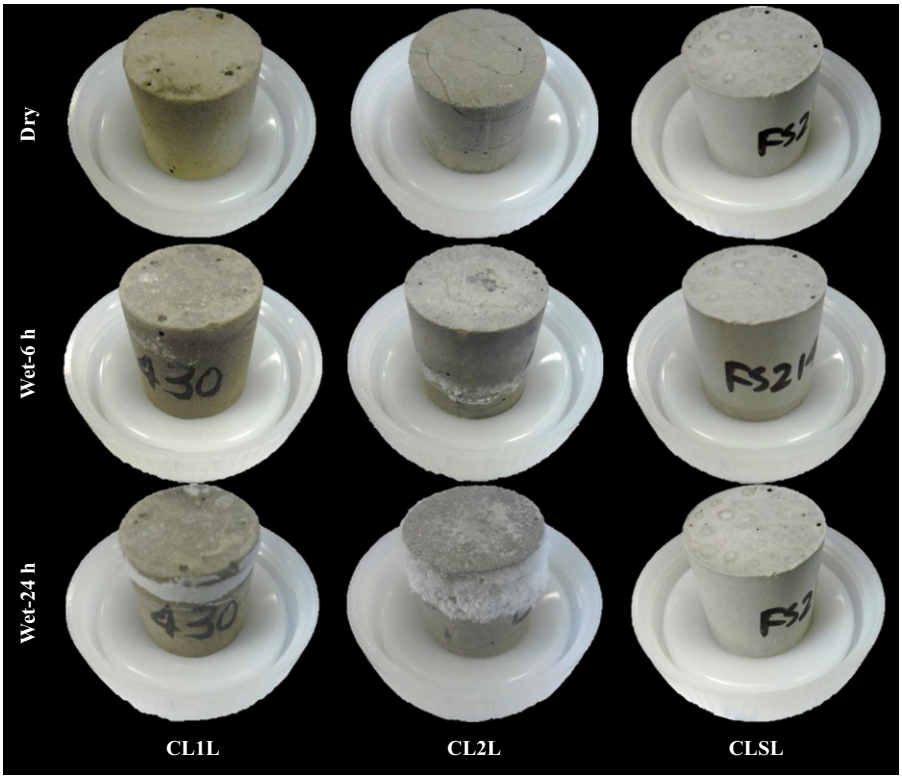

Fig. 3. Efflorescence of 23 °C sealed 90 d-aged geopolymer specimens when stored for times as marked with the bottom in contact with water.

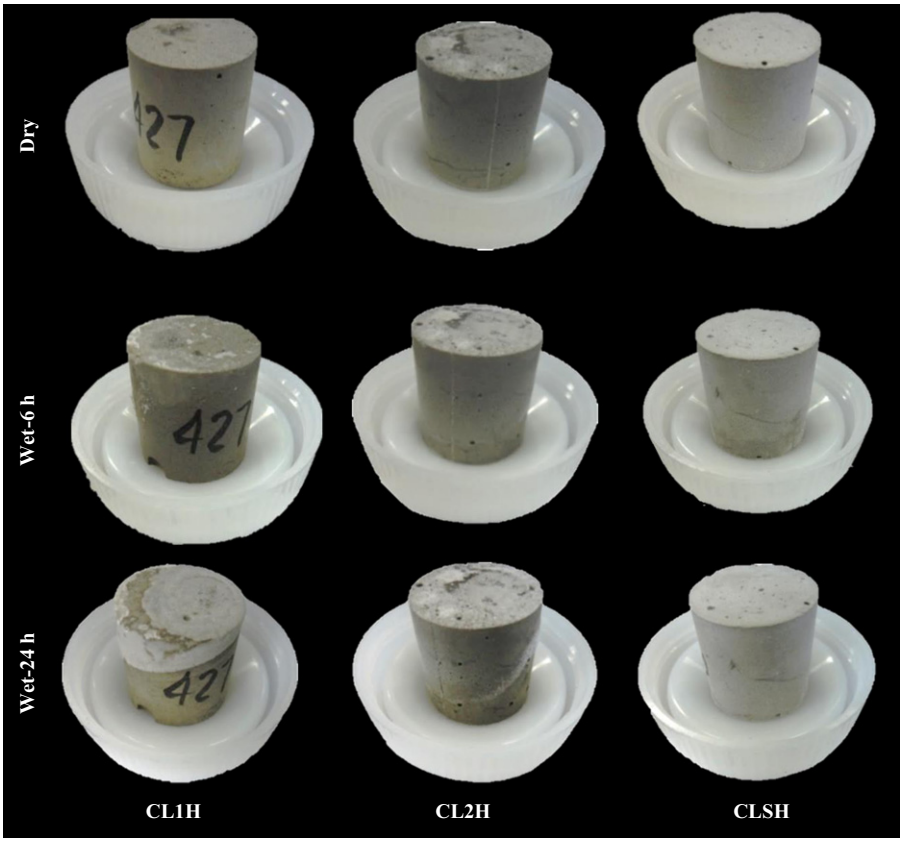

Fig. 4. Efflorescence of 80 °C hydrothermally 90 d-aged geopolymer specimens when stored for times as marked with the bottom in contact with water.

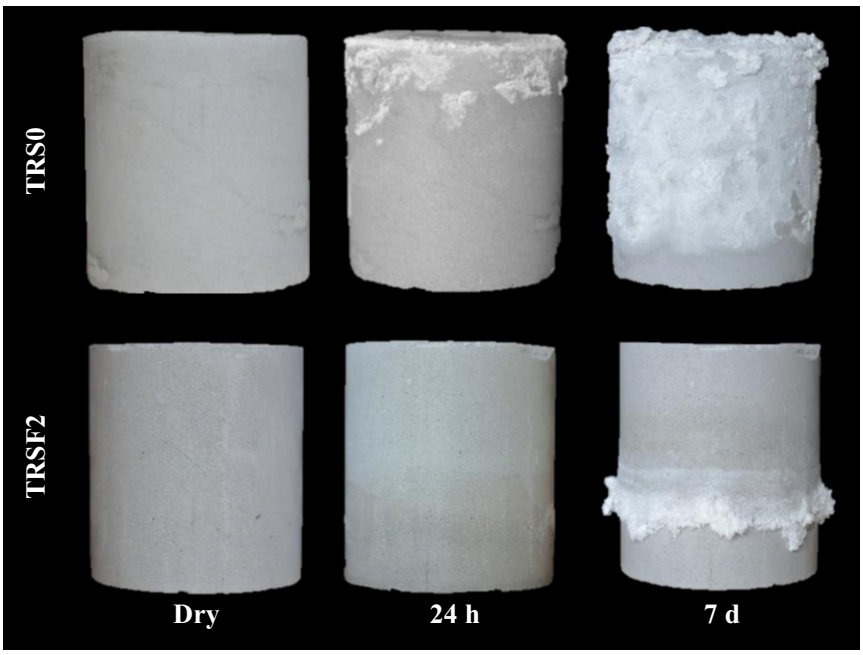

Fig. 5. Efflorescence of the dense geopolymer TRSF0 and the foamed geopolymer TRSF2 specimens stored for times with the bottom in contact with water.

voids in the foam geopolymer materials appear to be too large to lead to effective capillary transport of water up from the reservoir at the base of the specimen, and so the deposition of large quantities of alkali carbonates does not take place at the top of the specimens. However, optical microscopy reveals that the efflorescence products have instead grown inside the macropores of the materials (Fig. 6). These deposits may be important as a product of alkali migration through the materials, and so it is suggested to use other analytical methods, in addition to direct observation, to quantify the efflorescence of foamed geopolymers.

To gain a better understanding of efflorescence mechanisms, the white particulate product grown on specimen CL2L was collected and studied by XRD. Fig. 7 shows that the efflorescence product is a hydrous alkali carbonate, $Na_2CO_3 \cdot 7H_2O$. Similar sodium carbonates, which may contain different amounts of structural H_2O depending on temperature and humidity [29], were reported by other researchers as geopolymer efflorescence products [13,14]. As the carbonate grows from inside pores towards the outside, it is not expected that there will be large differences between the products in the pores and on the surface.

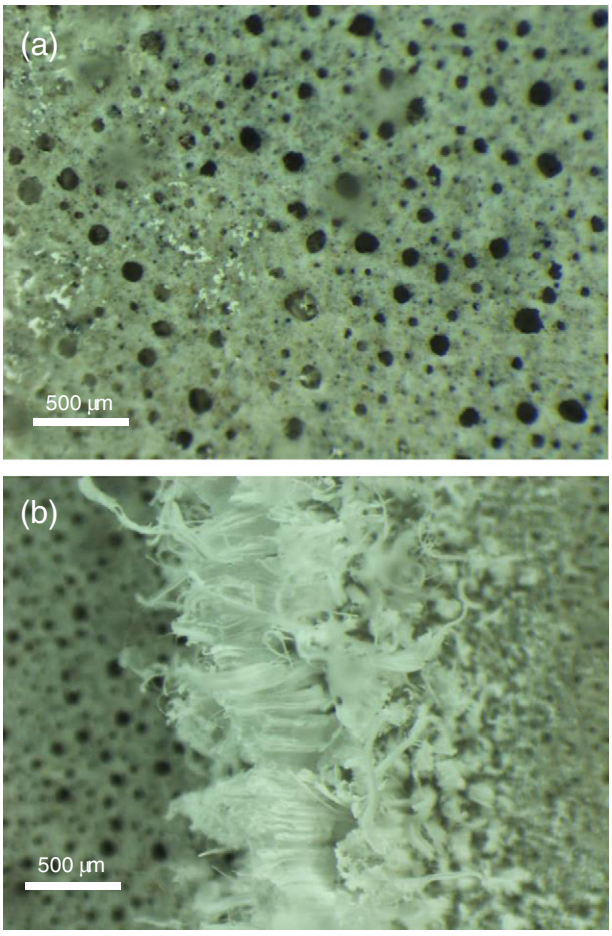

Fig. 6. Optical micrographs of the efflorescence products in the pores and on the surface of TRSF2 at 24 h (a) and 7 d (b).

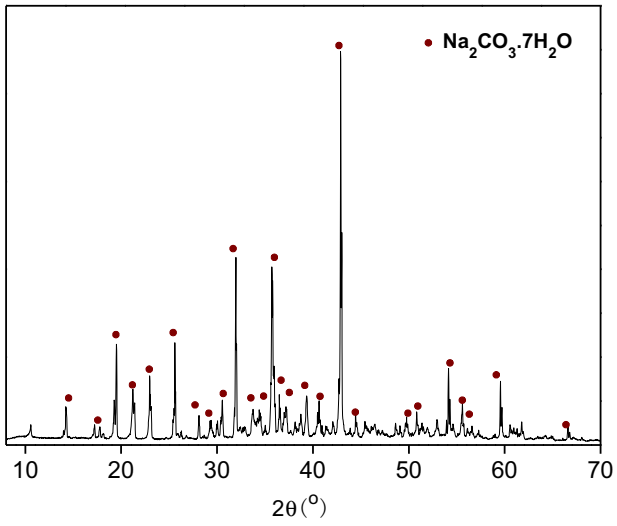

Fig. 7. XRD pattern of the efflorescence product scraped from the surface of geopolymer specimen CL2L.

Based on this observation, the mechanism of efflorescence formation can be sketched as follows:

$$CO_2(g) + 2OH^-(aq) \rightarrow CO_3^{2-}(aq) + H_2O$$

$$2Na^+(aq) + CO_3^{2-}(aq) + 7H_2O \rightarrow Na_2CO_3 \cdot 7H_2O\ (s).$$

This is therefore a partial neutralization process for alkaline geopolymers under natural carbonation conditions, as dissolved CO_2 acts as an acid and consumes hydroxides. The availability of mobile Na^+ and OH^- in geopolymer binders is the main reason for efflorescence in these materials. It is therefore proposed that leaching analysis may be able to provide more accurate and quantitative information regarding the efflorescence potential of the geopolymer samples.

3.2. Evaluation of the efflorescence potential by analysis of leachate

Fig. 8 presents the pH values of the leaching solutions of Callide fly ash geopolymers. In general, geopolymers prepared by hydrothermal ageing exhibit a lower leachate pH than those prepared by room temperature ageing in the early period of leaching. This indicates that the alkaline pore solution of the room temperature aged specimens is more accessible to the leaching process. After 24 h of leaching, the pH values in the leaching solutions of hydrothermally cured samples are lower than those of the room temperature cured samples, except for CL1H. Slag substitution provides some benefits in decreasing the leaching rate of OH^- in the early part of the test, but does not significantly change the leaching behaviour from a long term point of view, showing that the addition of slag provides pore filling effects, but does not actually lead to significant additional binding of alkalis in these mixes. The soluble silicate in the activator also does not provide any notable inhibition of OH^- leaching in the cases studied. The pH measurement results agree well with the efflorescence trends observed above.

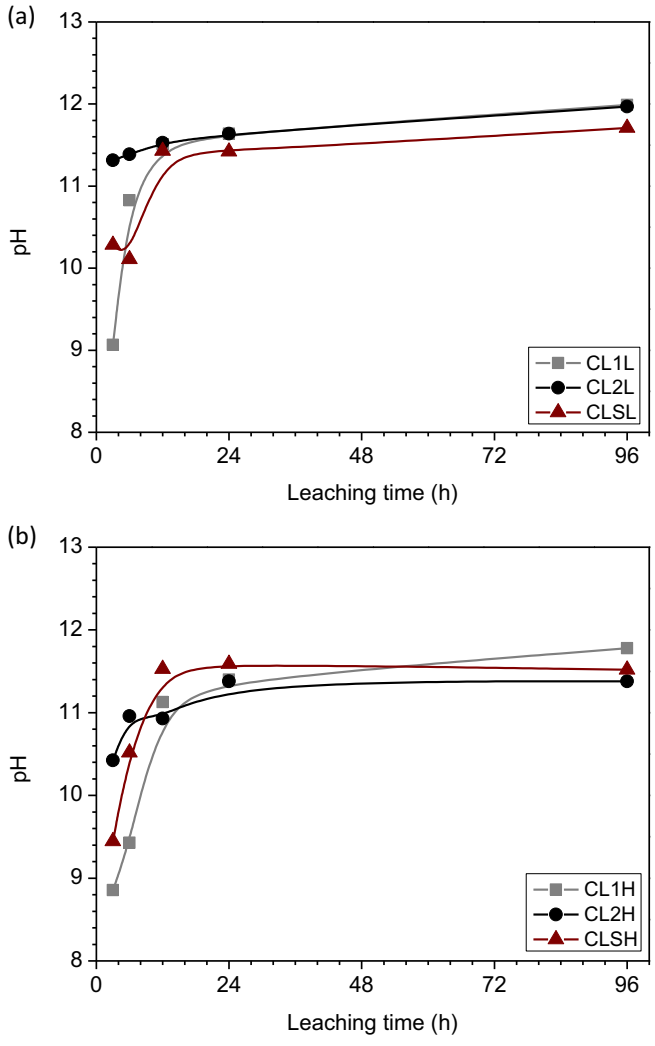

Fig. 8. The pH values of the leaching solutions of Callide geopolymer particles prepared by (a) sealed curing at 23 °C and (b) hydrothermal curing at 80 °C.

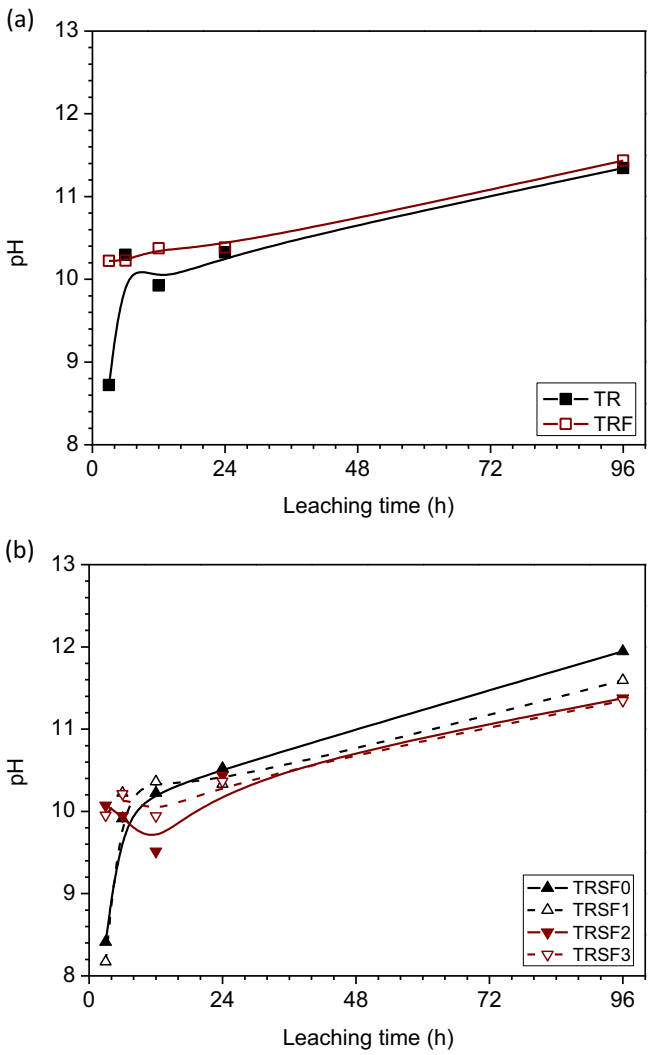

Fig. 9. The pH values of the leaching solutions of Tarong geopolymer particles: without slag addition (a) and with 30% slag addition (b).

Fig. 9 presents the pH values of the leaching solutions for solid and foamed Tarong geopolymers. For the specimens without slag substitution, foaming of the samples increases the initial leaching of OH^- in the first 3 h. Later, the foamed sample TRF exhibits a higher leaching rate than the equivalent dense sample TR. For the geopolymers with 30% slag addition, the higher porosity introduced increases initial OH^- leaching. In particular, comparing the leaching results of TRSF0 with TRSF2, the latter leaches more OH^- at the beginning, which means that the foamed samples show faster efflorescence than their solid counterparts, although this may not be able to be observed in the first hours by direct visual inspection. In general, the pH values are very similar after a long time of leaching for Callide and Tarong fly ash geopolymers, which is consistent with the fact that aluminosilicate

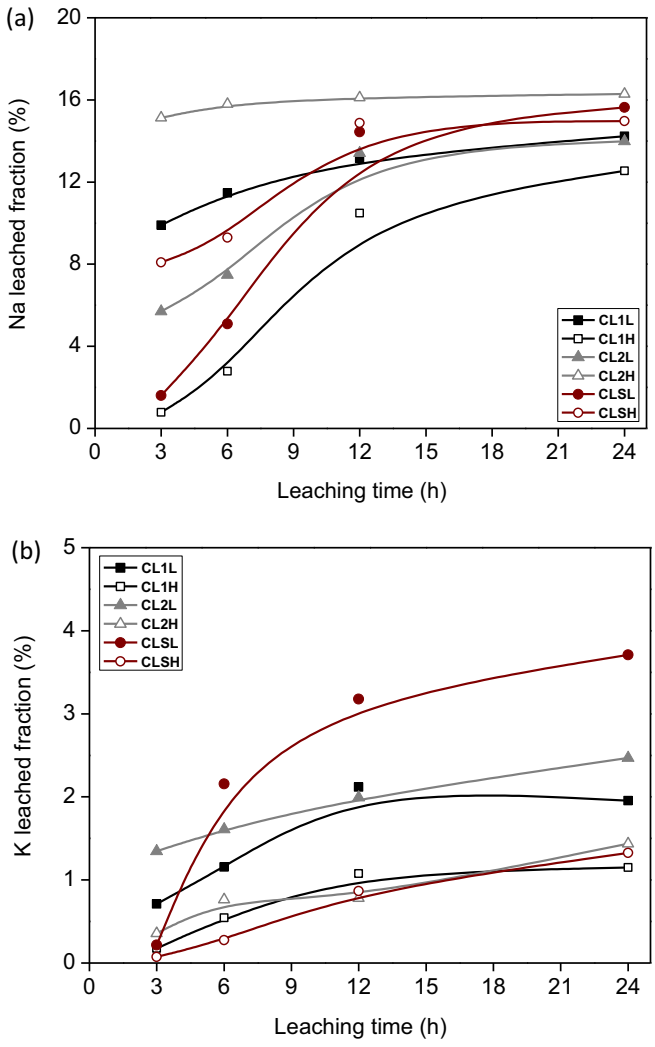

Fig. 10. The concentration of Na (a) and K (b) leached from the Callide geopolymers.

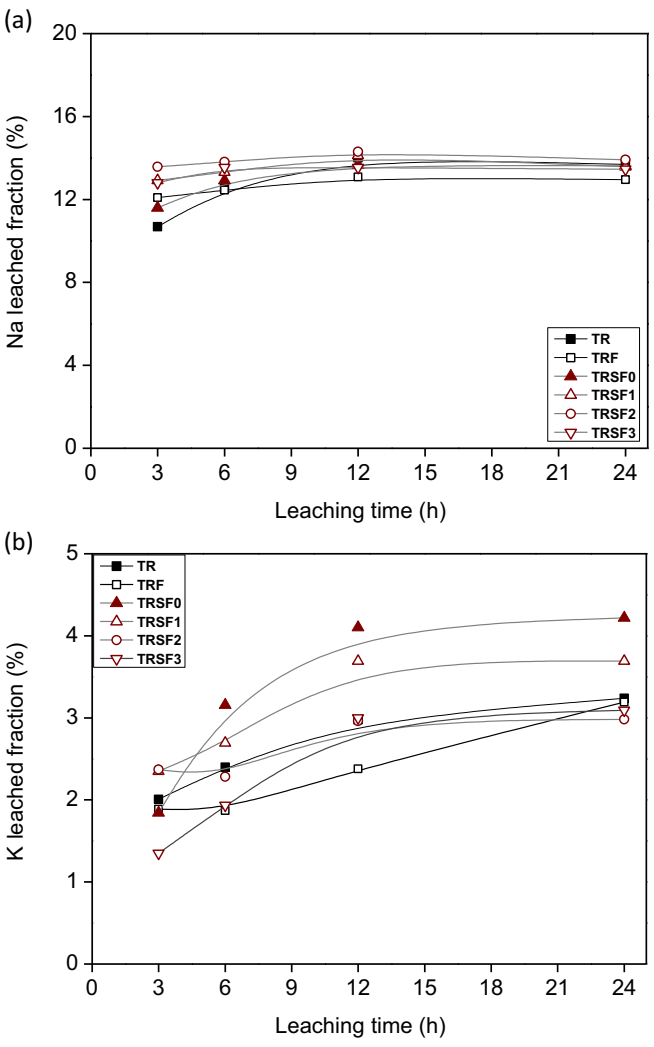

Fig. 11. The concentration of Na (a) and K (b) leached from the Tarong geopolymers.

gel chemistry and thus the degree of alkali binding are similar between the two ash sources.

Fig. 10 shows the Na and K concentrations in the leachate of Callide fly ash geopolymer samples as determined by AAS. The concentration of Na in the leachate was 100 to 150 ppm, which is around 100 times higher than the concentration of K. Any K present in the leachate must have been provided by the fly ash, as this was not contained in the activators used. For sodium silicate activated geopolymers, slag substitution reduces the total alkali leaching rate, but only has a positive effect in reducing the leaching amount in the hydrothermal cured samples. The hydrothermal ageing environment is helpful in reducing the initial alkali leaching rate, but has limited influence on the total alkali leaching. The leached fractions of Na and K both approach equilibrium after 24 h, and at similar rates, indicating that there do not seem to be significant differences in the leaching rates depending on the nature of the alkali, or whether it was originally supplied by the activators or the solid precursor. These leaching results are very consistent with the pH measurement results, except for CLSH, which leaches less alkalis but more OH^- than CLSL. Zheng et al. [30] found that their geopolymer cylinders released 40 to 60% of the total sodium after 45 h of immersion in acidic solution, which is much higher than the released fractions observed here, and this can be attributed to the use by those authors of an ash precursor containing a much lower content of reactive Si and Al for geopolymer formation, and probably also due to acidic solution attack.

Fig. 11 shows the Na and K leaching from Tarong ash samples, and all of the samples again show rapid initial Na leaching but then the establishment of an apparent equilibrium condition after this time. A minor difference between solid and foamed samples is observed that is the relatively slower leaching rate for TR and TRS than the foamed samples in the first 3 h, which is attributed to mass transport limitations in the more refined pores of the dense samples. The leaching behaviour of TR is very similar to CL1L, the corresponding ambient-cured dense sample made with Callide fly ash. The key reason for this is due to their very similar pore structures, as will be discussed in Section 3.4. The fraction of K leached from Tarong fly ash samples increases at a faster initial rate, but remains in the same range, as in the Callide fly ash geopolymers.

3.3. Compositional characteristics

It is likely that the efflorescence and alkali leaching rates of geopolymers are related at least in part to the nature of the mineral phases comprising the binders. The XRD analysis of Callide geopolymers (Fig. 12) shows that the major components in CL1L are amorphous, as reflected by the broad hump from 15 to 35° 2θ, with crystalline phases contributed by the fly ash; after 90 d of curing at 23 °C, the product consists of disordered geopolymeric gels and residual fly ash. The high temperature curing (80 °C, CL1H) promotes the transformation of gels into crystalline phases including analcime, ($NaAlSi_2O_6 \cdot H_2O$, ICSD#009357),

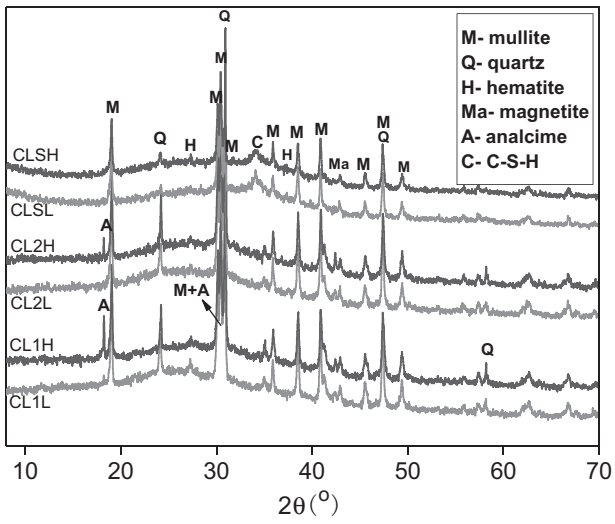

Fig. 12. XRD patterns of Callide geopolymers.

which has also been reported by other researchers [31,32]. The use of a soluble silicate activator, and/or the addition of slag, can hinder this transformation. The replacement of 20% of the fly ash by slag leads to the formation of poorly crystalline Al-substituted C–S–H gels (C–A–S–H) [33] as identified by the peak around 33° 2θ, and which may also show some degree of alkali substitution according to SEM–EDS analysis [20]. The dominant binder products in these mixes are still sodium aluminosilicate (N–A–S–H) gels, which are again more ordered in hydrothermally cured products as indicated by the increase in analcime peaks in samples cured at 80 °C. The influences of this structural change on efflorescence will be discussed in more detail in Section 4.

In geopolymers TR and TRS, the major reaction product phases are again amorphous (Fig. 13). The increased width of the broad diffraction 'hump' from 20° to 43° 2θ in the slag-containing TRSF samples is due to the partial reaction of the slag, as the remnant particles of this precursor contribute a hump at higher angle than the fly ash (Fig. 1). With the addition of 30% slag, minor amounts of C–A–S–H are again formed [34]. The characteristic peak attributed to C–A–S–H in the dense sample

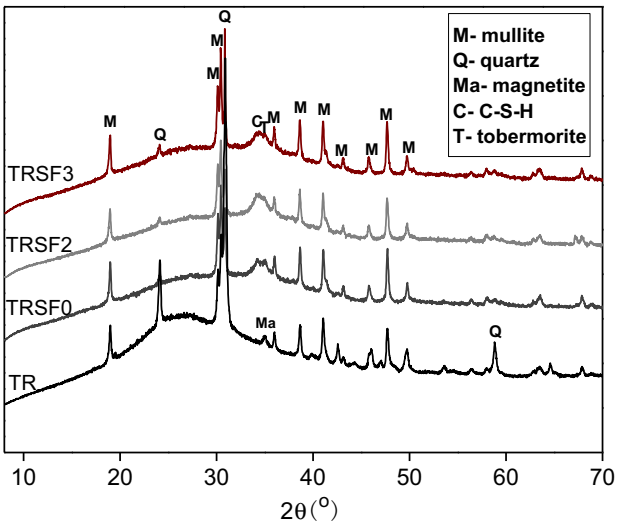

Fig. 13. XRD patterns of the solid Tarong geopolymer and the foamed samples containing 30% slag.

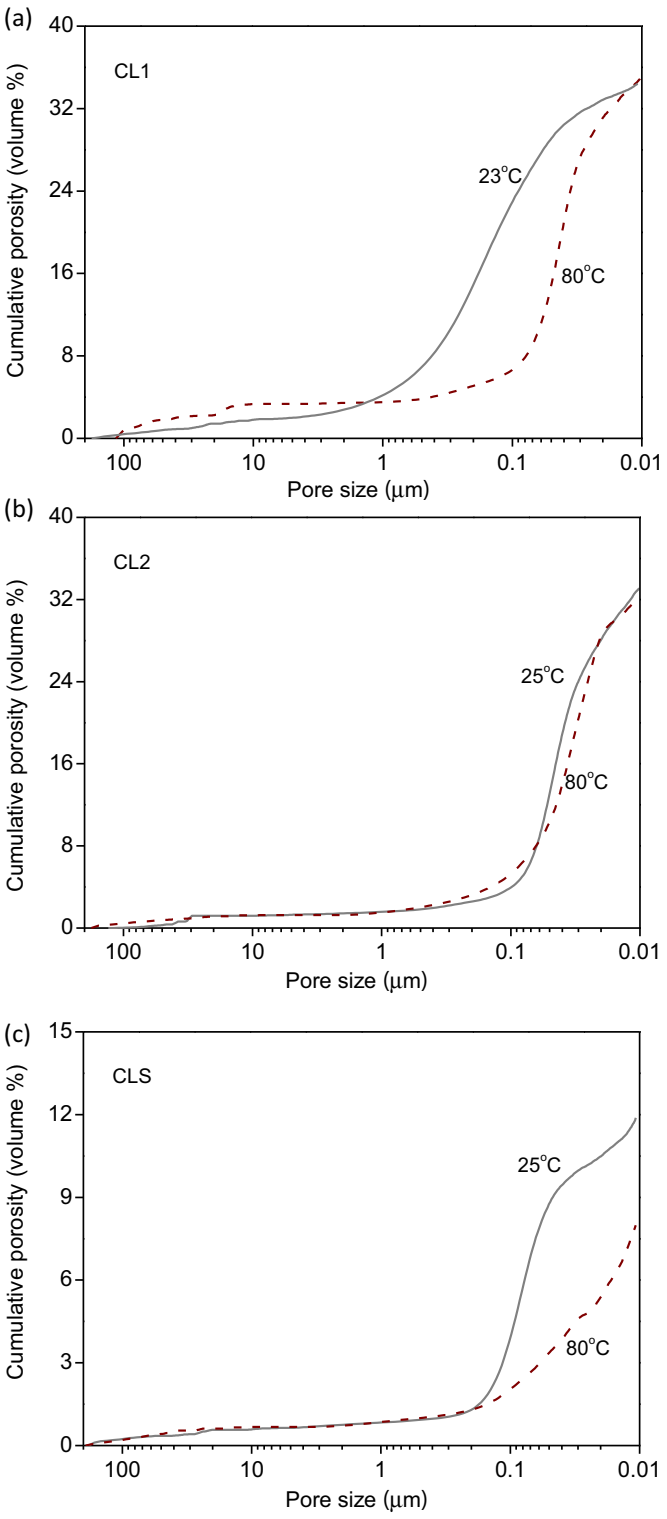

Fig. 14. Pore size distribution and porosity of Callide geopolymers by NaOH-activation (a), sodium silicate activation (b) and with 30% slag addition (c).

(TRSF0) is slightly sharper than in geopolymer foams, which is probably due to the slower evaporation of water from solid geopolymers, which provides a relatively longer hydration period for the slag. The diffraction patterns remain nearly constant as the foam dosage varies from 0 to 16% (Fig. 13), indicating that the influence of foam dosage on the mineralogy of aluminosilicate binder components is minimal.

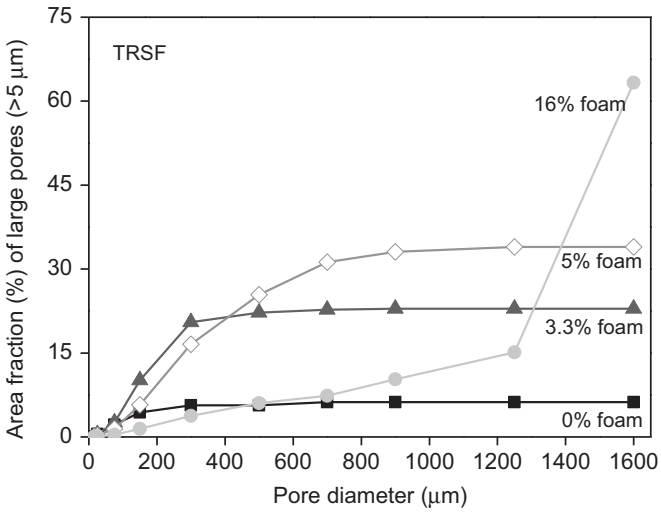

Fig. 15. The distribution of large pore (diameter >5 μm) in Tarong geopolymers as measured by image analysis.

3.4. Pore structure

Fig. 14 presents the measured pore size distribution of Callide fly ash geopolymers. The soluble silicate in the activator significantly reduces the volume of large pores (>100 nm), consistent with previous observations by SEM imaging in fly ash-based geopolymers [35]. Increasing the curing temperature reduces the pore sizes in all the three mixes, again consistent with the literature for fly ash-based geopolymers [36]. This could be one of the reasons that CL1H exhibits slower efflorescence than CL1L, and is also consistent with the much higher strength of this sample (Table 2). Slag substitution significantly reduces the mean pore size and also the total porosity, consistent with the literature [37], which is partially accounting for their slow efflorescence.

Fig. 15 shows the influence of foam addition on the macropore size distribution in Tarong fly ash geopolymers as measured by optical image analysis. As foam content increases, as expected, the area fraction (and thus volume) of large pores increases. In TRSF3, at 16% foam addition, most pores are >1 mm due to the higher degree of interconnection which takes place at their periphery. The large pores in the dense geopolymer TRSF0 are caused by air bubbles introduced in mixing, as well as a few holes where large residual fly ash particles were pulled out during sample preparation.

Fig. 16 shows the microstructure of Tarong geopolymers. In the dense sample TR, the pores are from the nano-scale up to several micrometres. Due to the large pores, which are connected by microcracks, the leaching solution is able to penetrate the sample easily. Therefore, the alkali cation leaching rate is fast in sample TR. In the foamed sample TRF, the large air voids similarly become channels for the mass transport in the geopolymers. Because of these large air voids, the positive effect of slag addition in decreasing efflorescence potential becomes very limited in these samples. The total porosities of the two batches of geopolymers are summarised in Table 3. The higher porosity of the two dense Tarong ash geopolymers (TR and TRS0) than the Callide ash samples is contributing to the faster alkali leaching, as is their larger pore size.

The water loss behaviour of geopolymers under TGA analysis conditions also provides some useful information in understanding the pore structure. As shown in Fig. 17, the weight loss of geopolymers can be divided into two main regions: from 25 to 300 °C, and from 300 to 890 °C [38]. In the first region the weight loss is due to the loss of free water and loosely bound water, which is relatively easily evaporated from gel pores. The weight loss in the second region is due to the loss of any structural water that is present in the form of –OH sites in geopolymeric gels, as well as any carbon introduced by the fly ash or the organic foaming agents, and also the carbonate content of any efflorescence products. For an identical activator dosage, the free water content changes significantly when curing temperature changes (Fig. 17a) or foam dosage changes (Fig. 17b). In the first region, CL1L loses much less water than CL1H, which is consistent with its much higher content of large pores (>1 μm). The water in large pores should be easily removed in the pre-conditioning of samples at 105 °C before analysis. CL2L and CL2H release similar quantities of water in both the first and second regions, which agrees well with their very similar porosity (Fig. 14b). Sample CLS loses much more mass in the region associated with free water than CL1 and CL2, which means that the alkali activation of slag changes the nature of the gel pores, and also the gel itself [39]. This means that the gel itself, and the gel pores, are holding pore liquids more tightly in slag-containing samples, which can also be confirmed by comparing the water loss of sample TRS (containing 30% slag) with TR

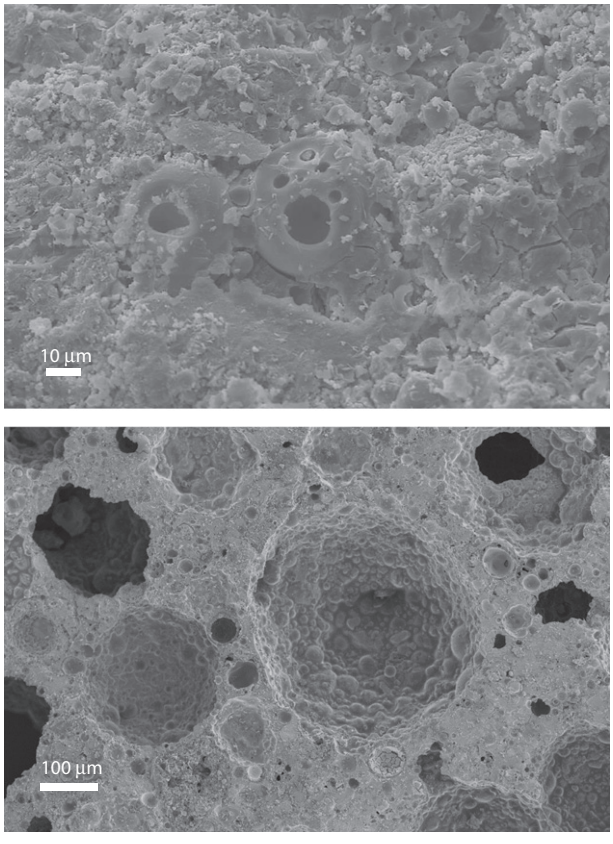

Fig. 16. SEM images of solid sample TR (a) and foamed sample TRS (b).

Table 3
Porosity of geopolymers as determined by MIP and water saturation.

Sample	MIP, %	Water saturation, %
CL1L	35.5	–
CL1H	34.4	–
CL2L	33.1	–
CL2H	31.8	–
CLSL	11.8	–
CLSH	8.0	–
TR	41.6	43.2
TRF	–	53.5
TRSF0	30.5	34.1
TRSF1	–	44.1
TRSF2	–	55.2
TRSF3	–	64.8

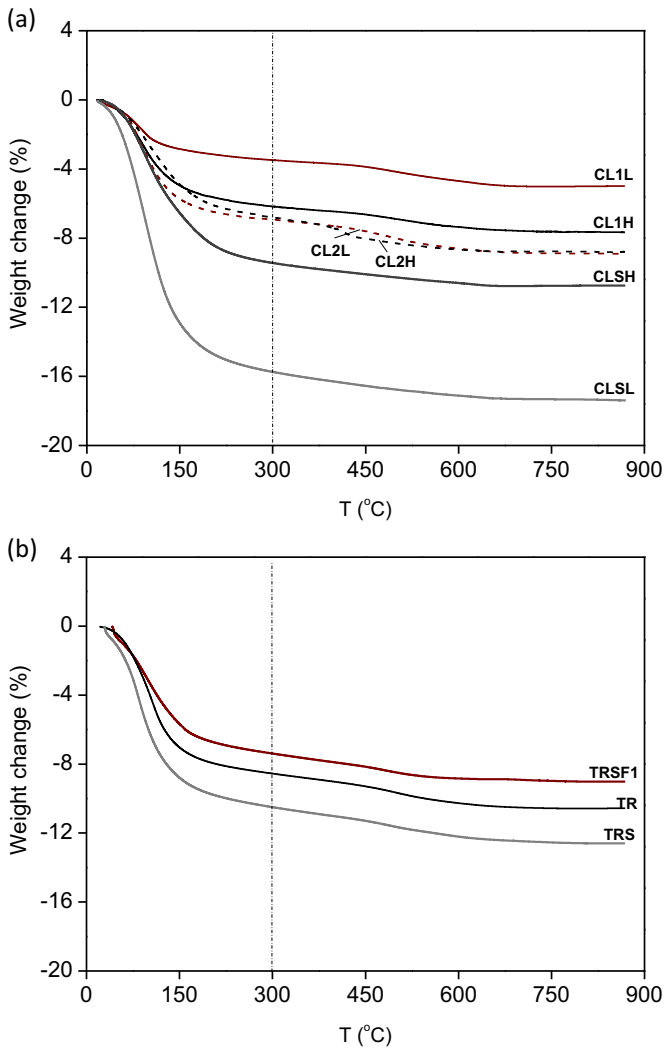

Fig. 17. Thermogravimetry data for Callide geopolymers (a) and Tarong geopolymers (b).

(100% fly ash). CL1L, CL2L and CL2L all lose water at lower temperatures than their corresponding high temperature cured samples, which is consistent with their coarser pore sizes. Foam addition increases the fraction of larger pores (Fig. 17b), so the evaporation of free water is easy in the sample pre-conditioning procedure before TGA analysis.

4. Discussion

The alkali content is certainly the most important compositional parameter influencing the efflorescence of geopolymers. It is expected that free alkalis will cause efflorescence under partially wet/partially dry conditions. However, the key problem is therefore the balance of how much alkali is optimal for a certain reaction system, as additional alkalis can often accelerate strength development and give a higher final strength, but also cause efflorescence. As one alkali cation is required to balance one negative framework charge due to Al(III) in four-coordination, any fly ash requires an optimal alkali content to match its reactive Al; noting that other elements such as Ca, Fe and Ti are also important in fly ash glass chemistry but are of secondary importance in the discussion here.

Given that the reactive Al in fly ash is mainly dissolved from glass phases (crystalline mullite dissolves much more slowly, if at all), the maximum optimal alkali content is able to be estimated as that which is required for to balance all of the Al present in the glass phases. In this study, the Callide fly ash contains 75.8 wt.% glass phases, containing 23.1 wt.% Al_2O_3, as determined by the Rietveld quantitative XRD method [24], and consistent with measurements on ashes from the same source by other researchers [17]. Based on this result, in 100 g of Callide fly ash the reactive Al_2O_3 content would be 0.23 mol, which requires 0.23 mol of Na_2O or 14.0 g to balance, for complete reaction of the fly ash. In this study, the Na_2O used was only 5.8 g, which was shown from the leaching results to still be in excess by 12–16%, depending on the curing conditions applied. Therefore, in practice, the process of selecting the real 'optimal' dosage of alkalis for a given fly ash-based geopolymer mix is complex, as it requires a balance between reducing efflorescence potential (and the cost associated with the alkaline activator, which is the most expensive component of a geopolymer mix [2]), and enhancing strength. This is most readily addressed by designing curing conditions to improve reaction extent as far as possible while keep the alkali content as low as possible. The geopolymerisation of fly ash has never been observed to reach complete reaction of the glassy ash components, even under 'optimal' reaction conditions; from the degree of alkali binding here, the extent of reaction of the fly ash glass can be estimated at 30–35%, assuming approximately congruent reaction of the different glassy phases present. Designing a geopolymer mix that is stoichiometrically matched to the expected (incomplete) degree of reaction is therefore recommended; this will lead to a lower reaction extent but will reduce the risk of efflorescence.

An alkali silicate activator is more favourable than an alkali hydroxide for achieving high strength geopolymers [40]. This is partially because of the higher volume of gels and the more compact microstructure achieved, as shown in Table 3 and Fig. 14(a, b). Pore solution analysis shows that as the soluble silicate content in a geopolymer mixture increases, the alkali metal concentration deceases [41]. This means that less alkali metal cations in pore solution tend to be released during leaching. However, from the efflorescence appearance shown in Figs. 3 and 4, the soluble silicate present in the activator has limited influence in efflorescence reduction. Instead, the efflorescence becomes even more intense at early times of exposure (<12 h). This is also evident when comparing the photographs of the samples with the data for leachability of OH^- and alkali metals (Figs. 8 & 10); the silicate-activated CL2L and CL2H leached more OH^- and alkali metal cations in the first 12 h than did the hydroxide-activated CL1L and CL1H. The total leached alkali concentrations in the two room temperature cured specimens CL1L and CL2L are very similar, at 13%, which is higher than CL1H but lower than CL2H. The reason that CL2H leached more alkali cations, and faster, is probably due to its more disordered reaction product and porous microstructure in comparison with CL1H, as the crystalline analcime which is observed at higher concentration in the hydroxide-activated CL1H under hydrothermal curing conditions (Fig. 12) provides more direct scope for alkali binding than does a disordered gel. In general, the soluble silica present in the activator will promote the early age efflorescence of geopolymers under wet conditions for room temperature cured geopolymers, and has very little influence on the long term efflorescence potential.

Given the small differences in pore structures between CL2L and CL2H, it is expected that the transformation towards crystalline phases is helpful in reducing the efflorescence potential. Hydrothermal ageing or curing has been suggested in the past as an effective way to reduce efflorescence [21], but this was previously only linked to the higher extent of reaction achieved at higher temperature, rather than direct identification of crystallinity as being an important factor. The current study confirms the positive effect of hydrothermal treatment, and shows that both of these mechanisms are likely important. The higher reaction extent can be reflected by the lower pH (or OH^- concentration) in Fig. 8b than in Fig. 8a at equilibrium. Due to the higher reaction extent of raw materials in hydrothermally cured samples, it would be expected that more K should be leachable from CL1H, CL2H and CLSH, as more glass phases are transformed to gels, leaving the K in more readily available

positions (i.e. within the gel or in the pore solution). However, it is noted from Fig. 10b that all three of the hydrothermally cured samples leached less K than the corresponding room temperature cured samples, and this is attributed to the partial crystallisation of geopolymeric gels reducing alkali metal mobility. Some other evidences that may also support this mechanism can be obtained by comparing the almost complete leaching of alkali metals from geopolymeric gels after 150 d [42] with the much lower fractions released from analcime and zeolitic phases after 80 d at 100 °C in water [43].

In terms of the effects of pore structure, generally, a larger mean pore radius and/or higher total porosity will cause faster alkali leaching, and consequently faster efflorescence. Comparing CL2L and CLSL, the addition of slag reduces the porosity by 64% but the pore size distribution (Fig. 14b) seems very similar. In CLSL, the efflorescence is slower than in CL2L (Fig. 3), and the alkali leaching rate in CLSL is also much slower in the first 12 h (Fig. 10a). However, it should be noted that the porosity of CLSL (and CLSH) may be higher than the determined values because the mercury may not be able to intrude into the very fine pores (<6 nm for the MIP conditions used in this study) which are present in Ca-containing geopolymer binders [44]. When most pores are large and mass transport is relatively unhindered, the overall porosity becomes a less important factor in affecting the efflorescence potential, as can be seen in the foamed samples.

5. Conclusions

The efflorescence behaviour of fly ash-based geopolymers is strongly dependent on the alkali activator solution type, curing temperature and slag addition, as the composition and microstructure change when these factors are varied. At the same alkali content (in terms of Na_2O to solid precursor mass ratio), soluble silica present in the activator restricts the early age efflorescence of room temperature cured geopolymers, but promotes early age efflorescence at 80 °C. This is mainly because of the finer pore size distribution developed in room temperature cured samples than in 80 °C cured samples under these activation conditions. However, in general, hydrothermal curing is usually beneficial in decreasing the efflorescence rate, due to the local reorganisation and crystallisation of N–A–S–H gels. When slag is used to partially substitute fly ash in geopolymer synthesis as a source of Ca, the pore sizes and porosities are smaller than in non-slag containing samples with either room temperature or hydrothermal curing, which leads to a much lower efflorescence rate.

Conversely, for foamed geopolymer samples, the larger pore size distribution and higher overall porosity lead to faster alkali leaching and consequently faster efflorescence, although this is sometimes not immediately evident to visual inspection because the alkali carbonate crystals grow inside the pores instead of on the exterior surface of the sample. When most pores are large, the overall degree of porosity becomes a less important factor in determining the efflorescence potential. From a long term view of alkali diffusion and leaching, either the addition of soluble silicate in the activator or the addition of slag is shown to have limited influence on the overall efflorescence potential; they influence the rate but not the achievable extent of alkali movement. This is particularly clear for the room temperature cured samples tested. Partial crystallisation of geopolymer gels reduces their efflorescence potential through alkali binding in ordered framework aluminosilicate structures.

This work suggests several principles which can be applied in mitigating efflorescence of geopolymer materials by reducing alkali mobility through microstructural and chemical control. It also suggests that the combination of the direct observation of geopolymer samples under certain conditions and the leaching analysis of fractured particles is a very effective method to predict the efflorescence potential of geopolymers.

Acknowledgements

The financial support of this study by Halok (Haald0808) and the Australian Research Council through a linkage project (LP130101016) is acknowledged. The participation of JLP in this research was funded by the European Research Council under the European Union's Seventh Framework Programme (FP/2007–2013)/ERC Grant Agreement #335928.

References

[1] J.L. Provis, S.A. Bernal, Geopolymers and related alkali-activated materials, Annu. Rev. Mater. Res. 44 (2014), http://dx.doi.org/10.1146/annurev-matsci-070813-113515 (in press).
[2] B.C. McLellan, R.P. Williams, J. Lay, A. van Riessen, G.D. Corder, Costs and carbon emissions for geopolymer pastes in comparison to ordinary Portland cement, J. Clean. Prod. 19 (2011) 1080–1090.
[3] J.R. Yost, A. Radlińska, S. Ernst, M. Salera, Structural behavior of alkali activated fly ash concrete. Part 1: mixture design, material properties and sample fabrication, Mater. Struct. 46 (2013) 435–447.
[4] J.R. Yost, A. Radlińska, S. Ernst, M. Salera, N.J. Martignetti, Structural behavior of alkali activated fly ash concrete. Part 2: structural testing and experimental findings, Mater. Struct. 46 (2013) 449–462.
[5] M. Sofi, J.S.J. van Deventer, P.A. Mendis, G.C. Lukey, Engineering properties of inorganic polymer concretes (IPCs), Cem. Concr. Res. 37 (2007) 251–257.
[6] J.L. Provis, V. Bílek, A. Buchwald, K. Dombrowski-Daube, B. Varela, Durability and testing — physical processes, in: J.L. Provis, J.S.J. van Deventer (Eds.), Alkali-Activated Materials: State-of-the-Art Report, RILEM TC 224-AAM, Springer/RILEM, Dordrecht, 2014, pp. 277–307.
[7] W.D.A. Rickard, R. Williams, J. Temuujin, A. van Riessen, Assessing the suitability of three Australian fly ashes as an aluminosilicate source for geopolymers in high temperature applications, Mater. Sci. Eng. A 528 (2011) 3390–3397.
[8] G. Kovalchuk, P.V. Krivenko, Producing fire- and heat-resistance geopolymers, in: J.L. Provis, J.S.J. van Deventer (Eds.), Geopolymers: Structure, Processing, Properties and Industrial Applications, Woodhead, Cambridge, UK, 2009, pp. 227–266.
[9] T. Bakharev, Resistance of geopolymer materials to acid attack, Cem. Concr. Res. 35 (2005) 658–670.
[10] R.R. Lloyd, J.L. Provis, J.S.J. van Deventer, Acid resistance of inorganic polymer binders. 1. Corrosion rate, Mater. Struct. 45 (2012) 1–14.
[11] J.S.J. van Deventer, J.L. Provis, P. Duxson, Technical and commercial progress in the adoption of geopolymer cement, Miner. Eng. 29 (2012) 89–104.
[12] S.A. Bernal, V. Bílek, M. Criado, A. Fernández-Jiménez, E. Kavalerova, P.V. Krivenko, M. Palacios, A. Palomo, J.L. Provis, F. Puertas, R. San Nicolas, C. Shi, F. Winnefeld, Durability and testing — degradation via mass transport, in: J.L. Provis, J.S.J. van Deventer (Eds.), Alkali-Activated Materials: State-of-the-Art Report, RILEM TC 224-AAM, Springer/RILEM, Dordrecht, 2014, pp. 223–276.
[13] F. Škvára, L. Kopecký, V. Šmilauer, L. Alberovská, L. Vinšová, Aluminosilicate polymers — influence of elevated temperatures, efflorescence, Ceram.-Silikáty 53 (2009) 276–282.
[14] J. Temuujin, A. van Riessen, Effect of fly ash preliminary calcination on the properties of geopolymer, J. Hazard. Mater. 164 (2009) 634–639.
[15] H. Szklorzová, V. Bílek, Influence of alkali ions in the activator on the performance of alkali-activated mortars, in: V. Bílek, Z. Keršner (Eds.), The 3rd International Symposium on Non-Traditional Cement and Concrete. Brno, Czech Republic, 2008, pp. 777–784.
[16] F. Škvára, S. Pavlasová, L. Kopecký, L. Myšková, L. Alberovská, High temperature properties of fly ash-based geopolymers, in: V. Bílek, Z. Keršner (Eds.), The 3rd International Symposium on Non-Traditional Cement and Concrete. Brno, Czech Republic, 2008, pp. 741–750.
[17] L. Keyte, What's wrong with Tarong?, (PhD thesis) The Importance of Coal Fly Ash Glass Chemistry in Inorganic Polymer Synthesis, The University of Melbourne, Australia, 2008.
[18] E.I. Diaz–Loya, E.N. Allouche, S. Vaidya, Mechanical properties of fly-ash-based geopolymer concrete, ACI Mater. J. 108 (2011) 300–306.
[19] S. Kumar, R. Kumar, S.P. Mehrotra, Influence of granulated blast furnace slag on the reaction, structure and properties of fly ash based geopolymer, J. Mater. Sci. 45 (2010) 607–615.
[20] T. Yang, X. Yao, Z. Zhang, H. Wang, Mechanical property and structure of alkali-activated fly ash and slag blends, J.Sust. Cem.-Based Mater. 1 (2012) 167–178.
[21] E. Najafi Kani, A. Allahverdi, J.L. Provis, Efflorescence control in geopolymer binders based on natural pozzolan, Cem. Concr. Compos. 34 (2011) 25–33.
[22] S. Delair, R. Guyonnet, A. Govin, B. Guilhot, Study of efflorescence forming process on cementitious materials, in: F. Toutlemonde, K. Sakai, O.E. Gjørv, N. Banthia (Eds.), 5th International Conference on Concrete Under Severe Conditions: Environment and Loading, Tours, France, 2007.
[23] T.L. Weng, W.T. Lin, A. Cheng, Effect of metakaolin on strength and efflorescence quantity of cement-based composites, Sci. World J. (2013) 11 (Article ID 606524) http://www.hindawi.com/journals/tswj/2013/606524/.
[24] Z. Zhang, The Effects of Chemical and Physical Properties of Fly Ashes on the Manufacture of Geopolymer Foam Concretes, (PhD Thesis) The University of Southern Queensland, Australia, 2013.

[25] C. Gallé, Effect of drying on cement-based materials pore structure as identified by mercury intrusion porosimetry: a comparative study between oven-vacuum and freeze-drying, Cem. Concr. Res. 31 (2001) 1467–1477.
[26] J. Adolphs, M.J. Setzer, P. Heine, Changes in pore structure and mercury contact angle of hardened cement paste depending on relative humidity, Mater. Struct. 35 (2002) 477–486.
[27] Z. Zhang, H. Wang, X. Yao, Y. Zhu, Effects of halloysite in kaolin on the formation and properties of geopolymers, Cem. Concr. Compos. 34 (2012) 709–715.
[28] E.K.K. Nambiar, K. Ramamurthy, Air-void characterisation of foam concrete, Cem. Concr. Res. 37 (2007) 221–230.
[29] H.P. Eugster, Sodium carbonate–bicarbonate minerals as indicators of P_{CO_2}, J. Geophys. Res. 71 (1966) 3369–3377.
[30] L. Zheng, C. Wang, W. Wang, Y. Shi, X. Gao, Immobilization of MSWI fly ash through geopolymerization: effects of water-wash, Waste Manag. 31 (2011) 311–317.
[31] R.R. Lloyd, Accelerated ageing of geopolymers, in: J.L. Provis, J.S.J. van Deventer (Eds.), Geopolymers: Structure, Processing, Properties and Industrial Applications, Woodhead, Cambridge, UK, 2009, pp. 139–166.
[32] J.L. Provis, A. Fernández-Jiménez, E. Kamseu, C. Leonelli, A. Palomo, Binder chemistry — low-calcium alkali-activated materials, in: J.L. Provis, J.S.J. van Deventer (Eds.), Alkali-Activated Materials: State-of-the-Art Report, RILEM TC 224-AAM, Springer/RILEM, Dordrecht, 2014, pp. 93–123.
[33] I. Ismail, S.A. Bernal, J.L. Provis, R. San Nicolas, S. Hamdan, J.S.J. van Deventer, Modification of phase evolution in alkali-activated blast furnace slag by the incorporation of fly ash, Cem. Concr. Compos. 45 (2014) 125–135.
[34] M. Ben Haha, B. Lothenbach, G. Le Saout, F. Winnefeld, Influence of slag chemistry on the hydration of alkali-activated blast-furnace slag — part II: effect of Al_2O_3, Cem. Concr. Res. 42 (2012) 74–83.
[35] J.S.J. van Deventer, J.L. Provis, P. Duxson, G.C. Lukey, Reaction mechanisms in the geopolymeric conversion of inorganic waste to useful products, J. Hazard. Mater. 139 (2007) 506–513.
[36] Sindhunate, G.C. Lukey, H. Xu, J.S.J. van Deventer, Effect of curing temperature and silicate concentration on fly ash-based geopolymerization, Ind. Eng. Chem. Res. 45 (2006) 3559–3568.
[37] J.L. Provis, R.J. Myers, C.E. White, V. Rose, J.S.J. van Deventer, X-ray microtomography shows pore structure and tortuosity in alkali-activated binders, Cem. Concr. Res. 42 (2012) 855–864.
[38] J.L. Provis, R.M. Harrex, S.A. Bernal, P. Duxson, J.S.J. van Deventer, Dilatometry of geopolymers as a means of selecting desirable fly ash sources, J. Non. Cryst. Solids 358 (2012) 1930–1937.
[39] I. Ismail, S.A. Bernal, J.L. Provis, S. Hamdan, J.S.J. van Deventer, Drying-induced changes in the structure of alkali-activated pastes, J. Mater. Sci. 48 (2013) 3566–3577.
[40] J.L. Provis, P. Duxson, E. Kavalerova, P.V. Krivenko, Z. Pan, F. Puertas, J.S.J. van Deventer, Historical aspects and overview, in: J.L. Provis, J.S.J. van Deventer (Eds.), Alkali-Activated Materials: State-of-the-Art Report, RILEM TC 224-AAM, Springer/RILEM, Dordrecht, 2014, pp. 11–57.
[41] R.R. Lloyd, J.L. Provis, J.S.J. van Deventer, Pore solution composition and alkali diffusion in inorganic polymer cement, Cem. Concr. Res. 40 (2010) 1386–1392.
[42] F. Škvára, V. Šmilauer, P. Hlaváček, L. Kopecký, Z. CÍlová, A weak alkali bond in (N, K)–A–S–H gels: evidence from leaching and modeling, Ceram.-Silik 56 (2012) 374–382.
[43] Z. Klika, Z. Weiss, M. Mellini, Water leaching of alkaline metals, Al and Si from selected aluminosilicates, Acta Geodyn. Geomater. 2 (2005) 81–90.
[44] R.R. Lloyd, J.L. Provis, K.J. Smeaton, J.S.J. van Deventer, Spatial distribution of pores in fly ash-based inorganic polymer gels visualised by Wood's metal intrusion, Microporous Mesoporous Mater. 126 (2009) 32–39.